Fermilab-Pub-06/055-E

First Direct Two-Sided Bound on the B^0_s Oscillation Frequency

V.M. Abazov,[36] B. Abbott,[76] M. Abolins,[66] B.S. Acharya,[29] M. Adams,[52] T. Adams,[50] M. Agelou,[18] J.-L. Agram,[19] S.H. Ahn,[31] M. Ahsan,[60] G.D. Alexeev,[36] G. Alkhazov,[40] A. Alton,[65] G. Alverson,[64] G.A. Alves,[2] M. Anastasoaie,[35] T. Andeen,[54] S. Anderson,[46] B. Andrieu,[17] M.S. Anzelc,[54] Y. Arnoud,[14] M. Arov,[53] A. Askew,[50] B. Åsman,[41] A.C.S. Assis Jesus,[3] O. Atramentov,[58] C. Autermann,[21] C. Avila,[8] C. Ay,[24] F. Badaud,[13] A. Baden,[62] L. Bagby,[53] B. Baldin,[51] D.V. Bandurin,[36] P. Banerjee,[29] S. Banerjee,[29] E. Barberis,[64] P. Bargassa,[81] P. Baringer,[59] C. Barnes,[44] J. Barreto,[2] J.F. Bartlett,[51] U. Bassler,[17] D. Bauer,[44] A. Bean,[59] M. Begalli,[3] M. Begel,[72] C. Belanger-Champagne,[5] A. Bellavance,[68] J.A. Benitez,[66] S.B. Beri,[27] G. Bernardi,[17] R. Bernhard,[42] L. Berntzon,[15] I. Bertram,[43] M. Besançon,[18] R. Beuselinck,[44] V.A. Bezzubov,[39] P.C. Bhat,[51] V. Bhatnagar,[27] M. Binder,[25] C. Biscarat,[43] K.M. Black,[63] I. Blackler,[44] G. Blazey,[53] F. Blekman,[44] S. Blessing,[50] D. Bloch,[19] K. Bloom,[68] U. Blumenschein,[23] A. Boehnlein,[51] O. Boeriu,[56] T.A. Bolton,[60] F. Borcherding,[51] G. Borissov,[43] K. Bos,[34] T. Bose,[78] A. Brandt,[79] R. Brock,[66] G. Brooijmans,[71] A. Bross,[51] D. Brown,[79] N.J. Buchanan,[50] D. Buchholz,[54] M. Buehler,[82] V. Buescher,[23] S. Burdin,[51] S. Burke,[46] T.H. Burnett,[83] E. Busato,[17] C.P. Buszello,[44] J.M. Butler,[63] S. Calvet,[15] J. Cammin,[72] S. Caron,[34] W. Carvalho,[3] B.C.K. Casey,[78] N.M. Cason,[56] H. Castilla-Valdez,[33] S. Chakrabarti,[29] D. Chakraborty,[53] K.M. Chan,[72] A. Chandra,[49] D. Chapin,[78] F. Charles,[19] E. Cheu,[46] F. Chevallier,[14] D.K. Cho,[63] S. Choi,[32] B. Choudhary,[28] L. Christofek,[59] D. Claes,[68] B. Clément,[19] C. Clément,[41] Y. Coadou,[5] M. Cooke,[81] W.E. Cooper,[51] D. Coppage,[59] M. Corcoran,[81] M.-C. Cousinou,[15] B. Cox,[45] S. Crépé-Renaudin,[14] D. Cutts,[78] M. Ćwiok,[30] H. da Motta,[2] A. Das,[63] M. Das,[61] B. Davies,[43] G. Davies,[44] G.A. Davis,[54] K. De,[79] P. de Jong,[34] S.J. de Jong,[35] E. De La Cruz-Burelo,[65] C. De Oliveira Martins,[3] J.D. Degenhardt,[65] F. Déliot,[18] M. Demarteau,[51] R. Demina,[72] P. Demine,[18] D. Denisov,[51] S.P. Denisov,[39] S. Desai,[73] H.T. Diehl,[51] M. Diesburg,[51] M. Doidge,[43] A. Dominguez,[68] H. Dong,[73] L.V. Dudko,[38] L. Duflot,[16] S.R. Dugad,[29] A. Duperrin,[15] J. Dyer,[66] A. Dyshkant,[53] M. Eads,[68] D. Edmunds,[66] T. Edwards,[45] J. Ellison,[49] J. Elmsheuser,[25] V.D. Elvira,[51] S. Eno,[62] P. Ermolov,[38] J. Estrada,[51] H. Evans,[55] A. Evdokimov,[37] V.N. Evdokimov,[39] S.N. Fatakia,[63] L. Feligioni,[63] A.V. Ferapontov,[60] T. Ferbel,[72] F. Fiedler,[25] F. Filthaut,[35] W. Fisher,[51] H.E. Fisk,[51] I. Fleck,[23] M. Ford,[45] M. Fortner,[53] H. Fox,[23] S. Fu,[51] S. Fuess,[51] T. Gadfort,[83] C.F. Galea,[35] E. Gallas,[51] E. Galyaev,[56] C. Garcia,[72] A. Garcia-Bellido,[83] J. Gardner,[59] V. Gavrilov,[37] A. Gay,[19] P. Gay,[13] D. Gelé,[19] R. Gelhaus,[49] C.E. Gerber,[52] Y. Gershtein,[50] D. Gillberg,[5] G. Ginther,[72] N. Gollub,[41] B. Gómez,[8] K. Gounder,[51] A. Goussiou,[56] P.D. Grannis,[73] H. Greenlee,[51] Z.D. Greenwood,[61] E.M. Gregores,[4] G. Grenier,[20] Ph. Gris,[13] J.-F. Grivaz,[16] S. Grünendahl,[51] M.W. Grünewald,[30] F. Guo,[73] J. Guo,[73] G. Gutierrez,[51] P. Gutierrez,[76] A. Haas,[71] N.J. Hadley,[62] P. Haefner,[25] S. Hagopian,[50] J. Haley,[69] I. Hall,[76] R.E. Hall,[48] L. Han,[7] K. Hanagaki,[51] K. Harder,[60] A. Harel,[72] R. Harrington,[64] J.M. Hauptman,[58] R. Hauser,[66] J. Hays,[54] T. Hebbeker,[21] D. Hedin,[53] J.G. Hegeman,[34] J.M. Heinmiller,[52] A.P. Heinson,[49] U. Heintz,[63] C. Hensel,[59] G. Hesketh,[64] M.D. Hildreth,[56] R. Hirosky,[82] J.D. Hobbs,[73] B. Hoeneisen,[12] M. Hohlfeld,[16] S.J. Hong,[31] R. Hooper,[78] P. Houben,[34] Y. Hu,[73] V. Hynek,[9] I. Iashvili,[70] R. Illingworth,[51] A.S. Ito,[51] S. Jabeen,[63] M. Jaffré,[16] S. Jain,[76] V. Jain,[74] K. Jakobs,[23] C. Jarvis,[62] A. Jenkins,[44] R. Jesik,[44] K. Johns,[46] C. Johnson,[71] M. Johnson,[51] A. Jonckheere,[51] P. Jonsson,[44] A. Juste,[51] D. Käfer,[21] S. Kahn,[74] E. Kajfasz,[15] A.M. Kalinin,[36] J.M. Kalk,[61] J.R. Kalk,[66] S. Kappler,[21] D. Karmanov,[38] J. Kasper,[63] I. Katsanos,[71] D. Kau,[50] R. Kaur,[27] R. Kehoe,[80] S. Kermiche,[15] S. Kesisoglou,[78] A. Khanov,[77] A. Kharchilava,[70] Y.M. Kharzheev,[36] D. Khatidze,[71] H. Kim,[79] T.J. Kim,[31] M.H. Kirby,[35] B. Klima,[51] J.M. Kohli,[27] J.-P. Konrath,[23] M. Kopal,[76] V.M. Korablev,[39] J. Kotcher,[74] B. Kothari,[71] A. Koubarovsky,[38] A.V. Kozelov,[39] J. Kozminski,[66] A. Kryemadhi,[82] S. Krzywdzinski,[51] T. Kuhl,[24] A. Kumar,[70] S. Kunori,[62] A. Kupco,[11] T. Kurča,[20,*] J. Kvita,[9] S. Lager,[41] S. Lammers,[71] G. Landsberg,[78] J. Lazoflores,[50] A.-C. Le Bihan,[19] P. Lebrun,[20] W.M. Lee,[53] A. Leflat,[38] F. Lehner,[42] C. Leonidopoulos,[71] V. Lesne,[13] J. Leveque,[46] P. Lewis,[44] J. Li,[79] Q.Z. Li,[51] J.G.R. Lima,[53] D. Lincoln,[51] J. Linnemann,[66] V.V. Lipaev,[39] R. Lipton,[51] Z. Liu,[5] L. Lobo,[44] A. Lobodenko,[40] M. Lokajicek,[11] A. Lounis,[19] P. Love,[43] H.J. Lubatti,[83] M. Lynker,[56] A.L. Lyon,[51] A.K.A. Maciel,[2] R.J. Madaras,[47] P. Mättig,[26] C. Magass,[21] A. Magerkurth,[65] A.-M. Magnan,[14] N. Makovec,[16] P.K. Mal,[56] H.B. Malbouisson,[3] S. Malik,[68] V.L. Malyshev,[36] H.S. Mao,[6] Y. Maravin,[60] M. Martens,[51] S.E.K. Mattingly,[78] R. McCarthy,[73] R. McCroskey,[46] D. Meder,[24] A. Melnitchouk,[67] A. Mendes,[15] L. Mendoza,[8] M. Merkin,[38] K.W. Merritt,[51] A. Meyer,[21] J. Meyer,[22] M. Michaut,[18] H. Miettinen,[81] T. Millet,[20] J. Mitrevski,[71] J. Molina,[3] N.K. Mondal,[29] J. Monk,[45] R.W. Moore,[5] T. Moulik,[59] G.S. Muanza,[16] M. Mulders,[51] M. Mulhearn,[71] L. Mundim,[3] Y.D. Mutaf,[73] E. Nagy,[15]

M. Naimuddin,[28] M. Narain,[63] N.A. Naumann,[35] H.A. Neal,[65] J.P. Negret,[8] S. Nelson,[50] P. Neustroev,[40]
C. Noeding,[23] A. Nomerotski,[51] S.F. Novaes,[4] T. Nunnemann,[25] V. O'Dell,[51] D.C. O'Neil,[5] G. Obrant,[40]
V. Oguri,[3] N. Oliveira,[3] N. Oshima,[51] R. Otec,[10] G.J. Otero y Garzón,[52] M. Owen,[45] P. Padley,[81] N. Parashar,[57]
S.-J. Park,[72] S.K. Park,[31] J. Parsons,[71] R. Partridge,[78] N. Parua,[73] A. Patwa,[74] G. Pawloski,[81] P.M. Perea,[49]
E. Perez,[18] K. Peters,[45] P. Pétroff,[16] M. Petteni,[44] R. Piegaia,[1] M.-A. Pleier,[22] P.L.M. Podesta-Lerma,[33]
V.M. Podstavkov,[51] Y. Pogorelov,[56] M.-E. Pol,[2] A. Pompoš,[76] B.G. Pope,[66] A.V. Popov,[39] W.L. Prado da Silva,[3]
H.B. Prosper,[50] S. Protopopescu,[74] J. Qian,[65] A. Quadt,[22] B. Quinn,[67] K.J. Rani,[29] K. Ranjan,[28] P.A. Rapidis,[51]
P.N. Ratoff,[43] P. Renkel,[80] S. Reucroft,[64] M. Rijssenbeek,[73] I. Ripp-Baudot,[19] F. Rizatdinova,[77] S. Robinson,[44]
R.F. Rodrigues,[3] C. Royon,[18] P. Rubinov,[51] R. Ruchti,[56] V.I. Rud,[38] G. Sajot,[14] A. Sánchez-Hernández,[33]
M.P. Sanders,[62] A. Santoro,[3] G. Savage,[51] L. Sawyer,[61] T. Scanlon,[44] D. Schaile,[25] R.D. Schamberger,[73]
Y. Scheglov,[40] H. Schellman,[54] P. Schieferdecker,[25] C. Schmitt,[26] C. Schwanenberger,[45] A. Schwartzman,[69]
R. Schwienhorst,[66] S. Sengupta,[50] H. Severini,[76] E. Shabalina,[52] M. Shamim,[60] V. Shary,[18] A.A. Shchukin,[39]
W.D. Shephard,[56] R.K. Shivpuri,[28] D. Shpakov,[64] V. Siccardi,[19] R.A. Sidwell,[60] V. Simak,[10] V. Sirotenko,[51]
P. Skubic,[76] P. Slattery,[72] R.P. Smith,[51] G.R. Snow,[68] J. Snow,[75] S. Snyder,[74] S. Söldner-Rembold,[45] X. Song,[53]
L. Sonnenschein,[17] A. Sopczak,[43] M. Sosebee,[79] K. Soustruznik,[9] M. Souza,[2] B. Spurlock,[79] J. Stark,[14] J. Steele,[61]
K. Stevenson,[55] V. Stolin,[37] A. Stone,[52] D.A. Stoyanova,[39] J. Strandberg,[41] M.A. Strang,[70] M. Strauss,[76]
R. Ströhmer,[25] D. Strom,[54] M. Strovink,[47] L. Stutte,[51] S. Sumowidagdo,[50] A. Sznajder,[3] M. Talby,[15]
P. Tamburello,[46] W. Taylor,[5] P. Telford,[45] J. Temple,[46] B. Tiller,[25] M. Titov,[23] V.V. Tokmenin,[36] M. Tomoto,[51]
T. Toole,[62] I. Torchiani,[23] S. Towers,[43] T. Trefzger,[24] S. Trincaz-Duvoid,[17] D. Tsybychev,[73] B. Tuchming,[18]
C. Tully,[69] A.S. Turcot,[45] P.M. Tuts,[71] R. Unalan,[66] L. Uvarov,[40] S. Uvarov,[40] S. Uzunyan,[53] B. Vachon,[5]
P.J. van den Berg,[34] R. Van Kooten,[55] W.M. van Leeuwen,[34] N. Varelas,[52] E.W. Varnes,[46] A. Vartapetian,[79]
I.A. Vasilyev,[39] M. Vaupel,[26] P. Verdier,[20] L.S. Vertogradov,[36] M. Verzocchi,[51] F. Villeneuve-Seguier,[44] P. Vint,[44]
J.-R. Vlimant,[17] E. Von Toerne,[60] M. Voutilainen,[68,†] M. Vreeswijk,[34] H.D. Wahl,[50] L. Wang,[62] J. Warchol,[56]
G. Watts,[83] M. Wayne,[56] M. Weber,[51] H. Weerts,[66] N. Wermes,[22] M. Wetstein,[62] A. White,[79] D. Wicke,[26]
G.W. Wilson,[59] S.J. Wimpenny,[49] M. Wobisch,[51] J. Womersley,[51] D.R. Wood,[64] T.R. Wyatt,[45] Y. Xie,[78]
N. Xuan,[56] S. Yacoob,[54] R. Yamada,[51] M. Yan,[62] T. Yasuda,[51] Y.A. Yatsunenko,[36] K. Yip,[74] H.D. Yoo,[78]
S.W. Youn,[54] C. Yu,[14] J. Yu,[79] A. Yurkewicz,[73] A. Zatserklyaniy,[53] C. Zeitnitz,[26] D. Zhang,[51] T. Zhao,[83]
Z. Zhao,[65] B. Zhou,[65] J. Zhu,[73] M. Zielinski,[72] D. Zieminska,[55] A. Zieminski,[55] V. Zutshi,[53] and E.G. Zverev[38]
(DØ Collaboration)

[1] *Universidad de Buenos Aires, Buenos Aires, Argentina*
[2] *LAFEX, Centro Brasileiro de Pesquisas Físicas, Rio de Janeiro, Brazil*
[3] *Universidade do Estado do Rio de Janeiro, Rio de Janeiro, Brazil*
[4] *Instituto de Física Teórica, Universidade Estadual Paulista, São Paulo, Brazil*
[5] *University of Alberta, Edmonton, Alberta, Canada, Simon Fraser University, Burnaby, British Columbia, Canada,*
York University, Toronto, Ontario, Canada, and McGill University, Montreal, Quebec, Canada
[6] *Institute of High Energy Physics, Beijing, People's Republic of China*
[7] *University of Science and Technology of China, Hefei, People's Republic of China*
[8] *Universidad de los Andes, Bogotá, Colombia*
[9] *Center for Particle Physics, Charles University, Prague, Czech Republic*
[10] *Czech Technical University, Prague, Czech Republic*
[11] *Center for Particle Physics, Institute of Physics, Academy of Sciences of the Czech Republic, Prague, Czech Republic*
[12] *Universidad San Francisco de Quito, Quito, Ecuador*
[13] *Laboratoire de Physique Corpusculaire, IN2P3-CNRS, Université Blaise Pascal, Clermont-Ferrand, France*
[14] *Laboratoire de Physique Subatomique et de Cosmologie, IN2P3-CNRS, Universite de Grenoble 1, Grenoble, France*
[15] *CPPM, IN2P3-CNRS, Université de la Méditerranée, Marseille, France*
[16] *IN2P3-CNRS, Laboratoire de l'Accélérateur Linéaire, Orsay, France*
[17] *LPNHE, IN2P3-CNRS, Universités Paris VI and VII, Paris, France*
[18] *DAPNIA/Service de Physique des Particules, CEA, Saclay, France*
[19] *IReS, IN2P3-CNRS, Université Louis Pasteur, Strasbourg, France, and Université de Haute Alsace, Mulhouse, France*
[20] *Institut de Physique Nucléaire de Lyon, IN2P3-CNRS, Université Claude Bernard, Villeurbanne, France*
[21] *III. Physikalisches Institut A, RWTH Aachen, Aachen, Germany*
[22] *Physikalisches Institut, Universität Bonn, Bonn, Germany*
[23] *Physikalisches Institut, Universität Freiburg, Freiburg, Germany*
[24] *Institut für Physik, Universität Mainz, Mainz, Germany*
[25] *Ludwig-Maximilians-Universität München, München, Germany*
[26] *Fachbereich Physik, University of Wuppertal, Wuppertal, Germany*
[27] *Panjab University, Chandigarh, India*

[28]*Delhi University, Delhi, India*
[29]*Tata Institute of Fundamental Research, Mumbai, India*
[30]*University College Dublin, Dublin, Ireland*
[31]*Korea Detector Laboratory, Korea University, Seoul, Korea*
[32]*SungKyunKwan University, Suwon, Korea*
[33]*CINVESTAV, Mexico City, Mexico*
[34]*FOM-Institute NIKHEF and University of Amsterdam/NIKHEF, Amsterdam, The Netherlands*
[35]*Radboud University Nijmegen/NIKHEF, Nijmegen, The Netherlands*
[36]*Joint Institute for Nuclear Research, Dubna, Russia*
[37]*Institute for Theoretical and Experimental Physics, Moscow, Russia*
[38]*Moscow State University, Moscow, Russia*
[39]*Institute for High Energy Physics, Protvino, Russia*
[40]*Petersburg Nuclear Physics Institute, St. Petersburg, Russia*
[41]*Lund University, Lund, Sweden, Royal Institute of Technology and Stockholm University, Stockholm, Sweden, and Uppsala University, Uppsala, Sweden*
[42]*Physik Institut der Universität Zürich, Zürich, Switzerland*
[43]*Lancaster University, Lancaster, United Kingdom*
[44]*Imperial College, London, United Kingdom*
[45]*University of Manchester, Manchester, United Kingdom*
[46]*University of Arizona, Tucson, Arizona 85721, USA*
[47]*Lawrence Berkeley National Laboratory and University of California, Berkeley, California 94720, USA*
[48]*California State University, Fresno, California 93740, USA*
[49]*University of California, Riverside, California 92521, USA*
[50]*Florida State University, Tallahassee, Florida 32306, USA*
[51]*Fermi National Accelerator Laboratory, Batavia, Illinois 60510, USA*
[52]*University of Illinois at Chicago, Chicago, Illinois 60607, USA*
[53]*Northern Illinois University, DeKalb, Illinois 60115, USA*
[54]*Northwestern University, Evanston, Illinois 60208, USA*
[55]*Indiana University, Bloomington, Indiana 47405, USA*
[56]*University of Notre Dame, Notre Dame, Indiana 46556, USA*
[57]*Purdue University Calumet, Hammond, Indiana 46323, USA*
[58]*Iowa State University, Ames, Iowa 50011, USA*
[59]*University of Kansas, Lawrence, Kansas 66045, USA*
[60]*Kansas State University, Manhattan, Kansas 66506, USA*
[61]*Louisiana Tech University, Ruston, Louisiana 71272, USA*
[62]*University of Maryland, College Park, Maryland 20742, USA*
[63]*Boston University, Boston, Massachusetts 02215, USA*
[64]*Northeastern University, Boston, Massachusetts 02115, USA*
[65]*University of Michigan, Ann Arbor, Michigan 48109, USA*
[66]*Michigan State University, East Lansing, Michigan 48824, USA*
[67]*University of Mississippi, University, Mississippi 38677, USA*
[68]*University of Nebraska, Lincoln, Nebraska 68588, USA*
[69]*Princeton University, Princeton, New Jersey 08544, USA*
[70]*State University of New York, Buffalo, New York 14260, USA*
[71]*Columbia University, New York, New York 10027, USA*
[72]*University of Rochester, Rochester, New York 14627, USA*
[73]*State University of New York, Stony Brook, New York 11794, USA*
[74]*Brookhaven National Laboratory, Upton, New York 11973, USA*
[75]*Langston University, Langston, Oklahoma 73050, USA*
[76]*University of Oklahoma, Norman, Oklahoma 73019, USA*
[77]*Oklahoma State University, Stillwater, Oklahoma 74078, USA*
[78]*Brown University, Providence, Rhode Island 02912, USA*
[79]*University of Texas, Arlington, Texas 76019, USA*
[80]*Southern Methodist University, Dallas, Texas 75275, USA*
[81]*Rice University, Houston, Texas 77005, USA*
[82]*University of Virginia, Charlottesville, Virginia 22901, USA*
[83]*University of Washington, Seattle, Washington 98195, USA*

(Dated: March 15, 2006)

We report the first direct two-sided bound on the B_s^0 oscillation frequency using a large sample of B_s^0 semileptonic decays corresponding to approximately 1 fb^{-1} of integrated luminosity collected by the DØ experiment in 2002–2006 during Run II of the Fermilab Tevatron Collider. The flavor (i.e., B_s^0 or $\bar{B}_s^0$) of the B_s^0 meson at the time of production was found using an opposite-side tagging technique, and the flavor at the time of decay was determined from the charge of the muon in the partially reconstructed decay $B_s^0 \to \mu^+ D_s^- X$, $D_s^- \to \phi\pi^-$, $\phi \to K^+K^-$. A likelihood scan over the oscillation frequency, Δm_s, gives a most probable value of 19 ps^{-1} and a range of $17 < \Delta m_s < 21$ ps^{-1} at the 90% C.L. At $\Delta m_s = 19$ ps^{-1}, the amplitude method yields a result that deviates from the hypothesis of an oscillation amplitude of zero by 2.5 standard deviations, corresponding to a two-sided C.L. of 1%.

PACS numbers: 12.15.Ff, 12.15.Hh, 13.20.Jf, 14.40.Nd

The phenomenon of B_d^0-$\bar{B}_d^0$ meson oscillations [1] is well established [2], with a precisely measured oscillation frequency Δm_d. In the standard model (SM) this parameter is proportional to the combination $|V_{tb}^* V_{td}|^2$ of CKM matrix elements. Since the matrix element V_{ts} is larger than V_{td}, the expected frequency Δm_s of B_s^0-$\bar{B}_s^0$ oscillations is higher. As a result, these oscillations have not been observed by any previous experiment and the current 95% C.L. lower limit on Δm_s is 16.6 ps^{-1} [2]. A measurement of the ratio of this frequency to Δm_d would result in a reduction on the total uncertainty on the matrix element V_{td} and would provide important further constraints on the CKM unitarity triangle and the source of CP violation in the SM. If the SM is correct and if information from current limits on B_s^0 oscillations is not included, then global fits to the unitarity triangle favor $\Delta m_s = 20.9^{+4.5}_{-4.2}$ ps^{-1} [3].

In the B_s^0-$\bar{B}_s^0$ system there are two mass eigenstates, the heavier (lighter) one having mass M_H (M_L) and decay width Γ_H (Γ_L). Denoting $\Delta m_s = M_H - M_L$, $\Delta\Gamma_s = \Gamma_L - \Gamma_H$, $\Gamma = (\Gamma_L + \Gamma_H)/2$, the time dependent probability that an initial B_s^0 decays at time t as a $\bar{B}_s^0$ (or vice versa) is given by $P^{\text{osc}} = \Gamma e^{-\Gamma t}(1 - \cos \Delta m_s t)/2$ while the probability that an initial B_s^0 decays as a B_s^0 is $P^{\text{nos}} = \Gamma e^{-\Gamma t}(1 + \cos \Delta m_s t)/2$, assuming that $\Delta\Gamma_s/\Gamma_s$ is small and neglecting CP violation. In this Letter, we present a study of B_s^0-$\bar{B}_s^0$ oscillations carried out using a large sample of semileptonic B_s^0 decays collected by the DØ experiment at Fermilab in $p\bar{p}$ collisions at $\sqrt{s} = 1.96$ TeV. The data correspond to approximately 1 fb^{-1} of integrated luminosity. In $p\bar{p}$ collisions, b quarks and anti-quarks are almost always produced in pairs. B_s^0 mesons were selected via their decays [4] $B_s^0 \to \mu^+ D_s^- X$. Flavor tagging a b or $\bar{b}$ on the opposite side to the signal meson establishes the signal meson as a B_s^0 or a $\bar{B}_s^0$ at time $t = 0$. When this meson decays semileptonically at time t, the charge of the decay muon then determines whether it has oscillated or not, i.e., $B_s^0 \to \mu^+ X$ and $\bar{B}_s^0 \to \mu^- X$, permitting the extraction of Δm_s.

The DØ detector is described in detail elsewhere [5]. The central tracking, calorimeter and muon systems are the components most important to this analysis. The central tracking system consists of a silicon microstrip tracker (SMT) and a central fiber tracker (CFT), both located within a 2-T superconducting solenoidal magnet, providing charged particle tracking for pseudorapidities $|\eta| < 3$, where $\eta = -\ln[\tan(\theta/2)]$ and θ is the polar angle. The three liquid-argon/uranium calorimeters are housed in separate cryostats. A central section, lying outside the tracking system, covers up to $|\eta| = 1.1$ and two end calorimeters extend the coverage to $|\eta| \approx 4.0$. The muon system consists of a layer of tracking detectors and scintillation trigger counters in front of 1.8-T iron toroids, followed by two similar layers after the toroids and has pseudorapidity coverage $|\eta| < 2.0$ [6].

No explicit trigger requirement was made, although most of the sample was collected with single muon triggers. The measurement then begins with a reconstruction of the decay chain $B_s^0 \to \mu^+ D_s^- X$, $D_s^- \to \phi\pi^-$, $\phi \to K^+K^-$. Muons were required to have transverse momentum $p_T(\mu^+) > 2$ GeV/c and momentum $p(\mu^+) > 3$ GeV/c, to have signals in both the CFT and SMT, and to have measurements in at least two layers of the muon system. All reconstructed charged particles in the event were clustered into jets [7], and the D_s^- candidate was reconstructed from three tracks found in the same jet as the reconstructed muon. Oppositely charged particles with $p_T > 0.7$ GeV/c were assigned the kaon mass and were required to have an invariant mass $1.004 < M(K^+K^-) < 1.034$ GeV/c^2, consistent with that of a ϕ meson. The third track was required to have $p_T > 0.5$ GeV/c and charge opposite to that of the muon charge and was assigned the pion mass. The three tracks were required to have signals in the CFT and SMT and to form a common D_s^- vertex using the algorithm described in detail in Ref. [8]. To reduce combinatorial background, the D_s^- vertex was required to have a positive displacement in the transverse plane, relative to the $p\bar{p}$ collision point (or primary vertex), with at least 4σ significance. The cosine of the angle between the D_s^- momentum and the direction from the primary vertex to the D_s^- vertex was required to be greater than 0.9. The trajectories of the muon and D_s^- candidates were required to originate from a common B_s^0 vertex, and the $\mu^+ D_s^-$ system was required to have an invariant mass between 2.6 and 5.4 GeV/c^2.

To further improve B_s^0 signal selection, a likelihood ratio method [9] was utilized. Using background sidebands (B) and sideband-subtracted signal (S) distributions in the data, probability distribution functions (*pdf*s) were found for a number of discriminating variables. These variables were the helicity angle between the D_s^- and $K^\pm$ momenta in the ϕ center-of-mass frame, the isolation of the $\mu^+ D_s^-$ system, the χ^2 of the D_s^- vertex,

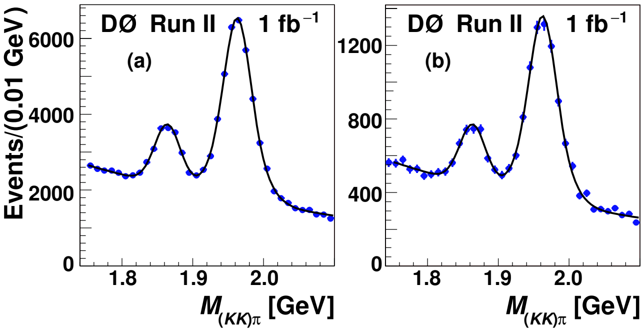

FIG. 1: $(K^+K^-)\pi^-$ invariant mass distribution for (a) the untagged B_s^0 sample, and (b) for candidates that have been flavor-tagged. The left and right peaks correspond to μ^+D^- and $\mu^+D_s^-$ candidates, respectively. The curve is a result of fitting a signal plus background model to the data. For fitting the mass spectra, a single Gaussian function was used to describe the $D^- \rightarrow \phi\pi^-$ decays and a double Gaussian was used for the $D_s^- \rightarrow \phi\pi^-$ decays. The background was modeled by an exponential function.

the invariant masses $M(\mu^+D_s^-)$ and $M(K^+K^-)$, and $p_T(K^+K^-)$. The final requirement on the combined selection likelihood ratio variable, $y_{\rm sel}$, was chosen to maximize the predicted ratio $S/\sqrt{S+B}$. The total number of D_s^- candidates after the above requirements is $N_{\rm tot} = 26{,}710 \pm 556\,({\rm stat})$ as shown in Fig. 1(a).

As described above, partial reconstruction of the b hadron on the opposite side to the B_s^0 gives information on the initial flavor of the B_s^0. The performance of the opposite-side flavor tagger (OST) [10] is characterized by the efficiency $\epsilon = N_{\rm tag}/N_{\rm tot}$, where $N_{\rm tag}$ is the number of tagged B_s^0 mesons; tag purity η_s, defined as $\eta_s = N_{\rm cor}/N_{\rm tag}$, where $N_{\rm cor}$ is the number of B_s^0 mesons with correct flavor identification; and the dilution $\mathcal{D}$, related to purity as $\mathcal{D} \equiv 2\eta_s - 1$. Again, a likelihood ratio method was used, where a set of flavor discriminating variables, $x_1, ... x_n$, was constructed for each event. In the construction of these variables, an object, either a lepton ℓ (electron or muon) or a reconstructed secondary vertex (SV), was defined to be on the opposite side from the B_s^0 meson if it satisfied $\cos\varphi(\vec{p}_{\ell \text{ or SV}}, \vec{p}_B) < 0.8$, where $\vec{p}_B$ is the reconstructed three-momentum of the B_s^0 meson, and φ is the azimuthal angle about the beam axis. A lepton jet charge was formed as $Q_J^\ell = \sum_i q^i p_T^i / \sum_i p_T^i$, where the sum is over all charged particles, including the lepton, inside a cone of $\Delta R = \sqrt{(\Delta\varphi)^2 + (\Delta\eta)^2} < 0.5$ centered on the lepton. Another discriminating variable is the secondary vertex charge, defined as $Q_{\rm SV} = \sum_i (q^i p_L^i)^{0.6} / \sum_i (p_L^i)^{0.6}$, where the sum is over all charged particles associated with the secondary vertex, and p_L^i is the longitudinal momentum of track i with respect to the direction of the secondary vertex momentum. Finally, event charge is defined as $Q_{\rm EV} = \sum_i q^i p_T^i / \sum_i p_T^i$ where the sum is over all tracks with $p_T > 0.5$ GeV/c outside a cone of $\Delta R > 1.5$ centered on the B_s^0 direction. The *pdf* of each discriminating variable was found in data for b and $\bar{b}$ quarks using a large sample of $B^+ \rightarrow \mu^+\nu\bar{D}^0$ events where the initial state is known from the charge of the decay muon.

For an initial b ($\bar{b}$) quark, the *pdf* for a given variable x_i is denoted $f_i^b(x_i)$ ($f_i^{\bar{b}}(x_i)$), and the combined tagging variable $d_{\rm tag}$ is defined as

$$d_{\rm tag} = \frac{1-z}{1+z}; \qquad z = \prod_{i=1}^{n} \frac{f_i^{\bar{b}}(x_i)}{f_i^b(x_i)}. \tag{1}$$

The variable $d_{\rm tag}$ varies between -1 and 1. An event with $d_{\rm tag} > 0$ (< 0) is tagged as a b ($\bar{b}$) quark.

Large samples of $B^+ \rightarrow \mu^+\nu\bar{D}^0X$ (non-oscillating) semileptonic candidates and $B_d^0 \rightarrow \mu^+\nu D^{*-}X$ (slowly oscillating) candidates were used with the described flavor tagger to measure $\Delta m_d = 0.506 \pm 0.020\,({\rm stat}) \pm 0.016\,({\rm syst})$ ps^{-1} [10], in good agreement with the world average value of 0.509 ± 0.004 ps^{-1} [2]. In addition, the latter value of Δm_d was used as an input to determine the purity and dilution of the OST for use in the B_s^0 mixing analysis. Splitting the sample into bins according to the tagging variable $|d_{\rm tag}|$ and measuring the tagging power $\epsilon\mathcal{D}^2$ as the sum of the tagging power in all bins, a value of $\epsilon\mathcal{D}^2 = [2.48 \pm 0.21\,({\rm stat})^{+0.08}_{-0.06}\,({\rm syst})]\%$ was obtained. To be able to use an event-by-event estimate of dilution when the OST is used to search for B_s^0 oscillations, the estimated dilution, $\mathcal{D}$, as a function of the $|d_{\rm tag}|$ was determined by measuring B_d^0 oscillations in bins of $|d_{\rm tag}|$ and parametrizing $\mathcal{D}$ with a third-order polynomial for $|d_{\rm tag}| < 0.6$. For $|d_{\rm tag}| > 0.6$, $\mathcal{D}$ is fixed to 0.6.

The OST was applied to the $B_s^0 \rightarrow \mu^+D_s^-X$ data sample, yielding $N_{\rm tag} = 5601 \pm 102\,({\rm stat})$ candidates having an identified initial state flavor as shown in Fig. 1(b). The tagging efficiency was $(20.9 \pm 0.7)\%$.

After flavor tagging, the proper decay time of candidates is needed; however, the undetected neutrino in the semileptonic B_s^0 decay does not allow a precise determination of the meson's momentum and Lorentz boost. This represents an important contribution to the smearing of the proper decay length in the semileptonic decays, in addition to the resolution effects. To take into account the effects of neutrinos and other missing particles, a K factor was estimated from Monte Carlo (MC) simulation by finding the distribution of $K = p_T(\mu^+D_s^-)/p_T(B)$ for a given decay channel. The proper decay length of each B_s^0 meson is then $ct(B_s^0) = l_M K$, where $l_M = M(B_s^0) \cdot (\vec{L}_T \cdot \vec{p}_T(\mu^+D_s^-))/(p_T(\mu^+D_s^-))^2$ is the measured visible proper decay length (VPDL), $\vec{L}_T$ is the vector from the primary vertex to the B_s^0 decay vertex in the transverse plane and $M(B_s^0) = 5.3696$ GeV/c^2 [1].

All flavor-tagged events with $1.72 < M(K^+K^-\pi^-) < 2.22$ GeV/c^2 were used in an unbinned fitting procedure. The likelihood, $\mathcal{L}$, for an event to arise from a specific source in the sample depends event-by-event on

l_M, its uncertainty σ_{l_M}, the invariant mass of the candidate $M(K^+K^-\pi^-)$, the predicted dilution $\mathcal{D}(d_{\rm tag})$, and the selection likelihood ratio variable $y_{\rm sel}$. The *pdf*s for each of these contributions, except for l_M, were determined from data. Four sources were considered: the signal $\mu^+D_s^-(\rightarrow\phi\pi^-)$; the accompanying peak due to $\mu^+D^-(\rightarrow\phi\pi^-)$; a small (less than 1%) reflection due to $\mu^+D^-(\rightarrow K^+\pi^-\pi^-)$, where the kaon mass is misassigned to one of the pions; and combinatorial background. The total fractions of the first two categories were determined from the mass fit of Fig. 1(b).

The $\mu^+D_s^-$ signal sample is composed mostly of B_s^0 mesons with some contributions from slowly oscillating B_d^0 mesons and non-oscillating B^+ mesons. Contributions of b baryons to the sample were estimated to be small and were neglected. The data were divided into subsamples with and without oscillation as determined by the OST. The distribution of the VPDL l for non-oscillated and oscillated cases was modeled appropriately for each type of B meson, e.g., for B_s^0:

$$p_s^{\rm nos/osc}(l,K,d_{\rm tag}) = \frac{K}{c\tau_{B_s^0}}\exp(-\frac{Kl}{c\tau_{B_s^0}})[1\pm\mathcal{D}(d_{\rm tag})\cos(\Delta m_s\cdot Kl/c)]/2. \quad (2)$$

The world averages [1] of $\tau_{B_d^0}$, τ_{B^+}, and Δm_d were used as inputs to the fit. The lifetime, $\tau_{B_s^0}$, was allowed to float in the fit. In the amplitude and likelihood scans described below, $\tau_{B_s^0}$ was fixed to this fitted value.

The total VPDL *pdf* for the $\mu^+D_s^-$ signal is then the sum over all decay channels, including branching fractions, that yield the D_s^- mass peak. The $B_s^0\rightarrow\mu^+\nu D_s^-X$ signal modes (including through D_s^{*-}, D_{s0}^{*-}, and $D_{s1}^{\prime -}$; and also μ^+ originating from τ^+ decay) comprise (85.6 ± 3.3)% of our sample, including reconstruction efficiency. Other backgrounds considered are decays via $B_s^0\rightarrow D_{(s)}^+D_s^-X$ and $\bar{B}_d^0, B^-\rightarrow DD_s^-$, followed by $D_{(s)}^+\rightarrow\mu^+\nu X$, with a real D_s^- reconstructed in the peak and an associated real μ^+. These backgrounds are not expected to oscillate with Δm_s. Another background taken into account occurs when the D_s^- meson originates from one b or c quark and the muon arises from another quark. This background peaks around the primary vertex (peaking backgrounds). The assigned uncertainty to each channel covers possible trigger efficiency biases. Translation from the true proper decay length, l, to the *measured* l_M, is achieved by a convolution of the VPDL detector resolution, of K factors over each normalized distribution for a given channel, and by including the reconstruction efficiency for a given channel as a function of VPDL.

The VPDL uncertainty was determined by the vertex fitting procedure, track parameters, and track parameter uncertainties. To account for possible mismodeling of detector uncertainties, resolution scale factors were introduced as determined by examining the pull distribution of the vertex positions of a sample of $J/\psi\rightarrow\mu^+\mu^-$ decays. Using these scale factors, the convolving function used for VPDL resolution was a double Gaussian function using $0.998\sigma_{l_M}$ for a fraction of 72% and $1.775\sigma_{l_M}$ for the remainder. To find the reconstruction efficiencies and the K-factor distributions for each channel in bins of $M(\mu^+D_s^-)$, a MC simulation was used that included the PYTHIA generator [11] interfaced with the EVTGEN decay package [12], followed by full GEANT [13] modeling of the detector response and event reconstruction. The reconstruction efficiency as a function of VPDL due to lifetime-dependent requirements was found for each channel using MC simulations, and as a cross check, the efficiency was also determined from the data by fixing $\tau_{B_s^0}$ and fitting for the functional form of the efficiency. The shape of the VPDL distribution for peaking backgrounds was also found from MC simulation, and the fraction from this source was allowed to float in the fit.

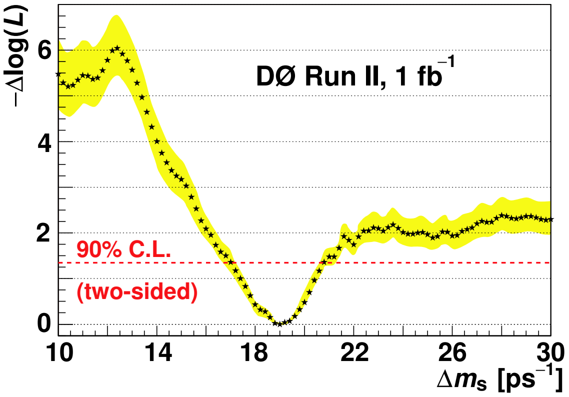

FIG. 2: Value of $-\Delta\log\mathcal{L}$ as a function of Δm_s. Star symbols do not include systematic uncertainties, and the shaded band represents the envelope of all $\log\mathcal{L}$ scan curves due to different systematic uncertainties.

Several contributions to the combinatorial background were considered which have different VPDL distributions. True prompt background was modeled with a Gaussian function with a separate scale factor on the width; background due to fake vertices around the primary vertices was modeled with another Gaussian function; and long-lived background was modeled with an exponential function convoluted with the resolution, including a component oscillating with a frequency of Δm_d. The unbinned fit of the total tagged sample was used to determine the various fractions of signal and backgrounds and the background VPDL parameterizations. The fitted value of the B_s^0 lifetime agrees with expectations.

Figure 2 shows the value of $-\Delta\log\mathcal{L}$ as a function of Δm_s, indicating a favored value of 19 ps^{-1}, while variation of $-\log\mathcal{L}$ from the minimum indicates an oscillation frequency of $17<\Delta m_s<21$ ps^{-1} at the 90% C.L. The uncertainties are approximately Gaussian inside this interval. Using 1000 parametrized MC samples with sim-

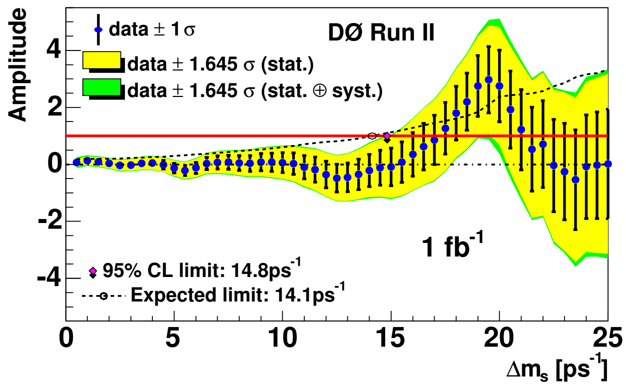

FIG. 3: B_s^0 oscillation amplitude as a function of oscillation frequency, Δm_s. The red (solid) line shows the $\mathcal{A} = 1$ axis for reference. The dashed line shows the expected limit including both statistical and systematic uncertainties.

ilar statistics, VPDL resolution, overall tagging performance, and sample composition of the data sample, it was determined that for a true value of $\Delta m_s = 19$ ps^{-1}, the probability was 15% for measuring a value in the range $17 < \Delta m_s < 21$ ps^{-1} with a $-\Delta \log \mathcal{L}$ lower by at least 1.9 than the corresponding value at $\Delta m_s = 25$ ps^{-1}. The plateau of the likelihood curve shows the region where we do not have sufficient resolution to measure an oscillation, and if the true value of Δm_s is in this region, our measured confidence interval does not make any statement about the frequency.

The amplitude method [14], a standard method for combining experimental oscillation limits, was also used. Equation 2 was modified to include the oscillation amplitude $\mathcal{A}$ as an additional coefficient on the $\cos(\Delta m_s \cdot Kl/c)$ term. The unbinned fit was repeated for fixed input values of Δm_s and the fitted value of $\mathcal{A}$ and its uncertainty $\sigma_{\mathcal{A}}$ found for each step as shown in Fig. 3. At $\Delta m_s = 19$ ps^{-1} the measured data point deviates from the hypothesis $\mathcal{A} = 0$ ($\mathcal{A} = 1$) by 2.5 (1.6) standard deviations, corresponding to a two-sided C.L. of 1% (10%), and is in agreement with the likelihood results. Parametrized MC tests indicate that, in the event of a signal, the amplitude method provides on average a less accurate determination of the value of Δm_s. In our case, this does not allow as precise a determination of the preferred Δm_s interval as does the likelihood method.

Systematic uncertainties were addressed by varying inputs, cut requirements, branching ratios, and *pdf* modeling. The branching ratios were varied within known uncertainties [1] and large variations taken for those not yet measured. The K-factor distributions were varied within uncertainties, using measured instead of generated momenta in the MC simulation, or smoothed. The fractions of peaking and combinatorial background were varied within uncertainties. Uncertainties in the levels of the reflections were considered. The functional form to determine the dilution $\mathcal{D}(d_{\rm tag})$ was varied. The lifetime $\tau_{B_s^0}$ was set to its world average value instead of being allowed to float, and $\Delta\Gamma_s$ was allowed to be non-zero. The scale factors on the signal and background resolutions were varied within uncertainties, and typically generated the largest systematic uncertainty in the region of interest. A separate scan of $-\Delta \log \mathcal{L}$ was taken for each variation, and the envelope of all such curves is indicated as the band on Fig. 2. The same systematic uncertainties were considered for the amplitude method using the procedure of Ref. [14], and when added in quadrature with the statistical uncertainties, represent a small effect as shown in Fig. 3. Taking these systematic uncertainties into account, from the amplitude method, we obtain an expected limit of 14.1 ps^{-1} and an observed lower limit on the frequency of $\Delta m_s > 14.8$ ps^{-1} at the 95% C.L., consistent with the likelihood scan.

To test the statistical significance of the observed minimum, an ensemble test using the data sample was performed by randomly assigning a flavor to each candidate while retaining all other information for the candidate, effectively simulating a B_s^0 oscillation with an infinite frequency. 5000 such experiments were performed and the change of $\log \mathcal{L}$ between $\Delta m_s = 25$ ps^{-1} and the minimum of $-\log \mathcal{L}$ was determined. For infinite frequency, the probability to observe a minimum in the range $16 < \Delta m_s < 22$ ps^{-1} with a decrease in $-\log \mathcal{L}$ with respect to the corresponding value at $\Delta m_s = 25$ ps^{-1} of more than 1.7, corresponding to our observation including systematic uncertainties, was found to be (5.0 ± 0.3)%. This range of Δm_s was chosen to encompass the world average lower limit and the edge of our sensitive region. Similar probabilities were found using ensembles of parameterized MC events.

A cross check was performed using the decays $B_d^0 \to X\mu^+ D^- (\to \phi\pi^-)$ present in the data sample (see Fig. 1). The peak amplitude is in good agreement with unity at $\Delta m_d \approx 0.5$ ps^{-1}, as expected for B_d^0-$\bar{B}_d^0$ oscillations, thus confirming the dilution calibration.

In summary, a study of B_s^0-$\bar{B}_s^0$ oscillations was performed using $B_s^0 \to \mu^+ D_s^- X$ decays, where $D_s^- \to \phi\pi^-$ and $\phi \to K^+K^-$, an opposite-side flavor tagging algorithm, and an unbinned likelihood fit. At $\Delta m_s = 19$ ps^{-1}, the amplitude method yields a result that deviates from the hypothesis $\mathcal{A} = 0$ ($\mathcal{A} = 1$) by 2.5 (1.6) standard deviations, corresponding to a two-sided C.L. of 1% (10%). For a more accurate determination of Δm_s, a likelihood scan has been performed with the amplitude set to one. The likelihood curve is well behaved near a preferred value of 19 ps^{-1} with a 90% C.L. interval of $17 < \Delta m_s < 21$ ps^{-1}, assuming Gaussian uncertainties. The lower edge of the confidence level interval is near the world average 95% C.L. lower limit $\Delta m_s > 16.6$ ps^{-1} [2]. Ensemble tests indicate that if Δm_s lies above the sensitive region, i.e., above approximately 22 ps^{-1}, there is a $(5.0 \pm 0.3)\%$ probability that it would produce a likelihood minimum similar to the one observed in the interval $16 < \Delta m_s < 22\ \mathrm{ps}^{-1}$. This is the first report of a direct two-sided bound on the B_s^0 oscillation frequency.

We thank the staffs at Fermilab and collaborating institutions, and acknowledge support from the DOE and NSF (USA); CEA and CNRS/IN2P3 (France); FASI, Rosatom and RFBR (Russia); CAPES, CNPq, FAPERJ, FAPESP and FUNDUNESP (Brazil); DAE and DST (India); Colciencias (Colombia); CONACyT (Mexico); KRF and KOSEF (Korea); CONICET and UBACyT (Argentina); FOM (The Netherlands); PPARC (United Kingdom); MSMT (Czech Republic); CRC Program, CFI, NSERC and WestGrid Project (Canada); BMBF and DFG (Germany); SFI (Ireland); The Swedish Research Council (Sweden); Research Corporation; Alexander von Humboldt Foundation; and the Marie Curie Program.

---

[*] On leave from IEP SAS Kosice, Slovakia.

[†] Visitor from Helsinki Institute of Physics, Helsinki, Finland.

[1] S. Eidelman *et al.*, Phys. Lett. B **592**, 1 (2004).

[2] Heavy Flavor Averaging Group, "Averages of b-hadron properties at the end of 2005," arXiv:hep-ex/0603003. Note that we take $\hbar = c = 1$, hence the units on Δm_s.

[3] CKMfitter Group, J. Charles *et al.*, Eur. Phys. J. **C41**, 1 (2005).

[4] Charge conjugate states are assumed throughout.

[5] V. Abazov *et al.* [DØ Collaboration] "The Upgraded DØ Detector," submitted to Nucl. Instrum. Methods Phys. Res. A., arXiv:physics/0507191.

[6] V.M. Abazov *et al.*, Nucl. Instrum. Meth. Phys. Res. A **552**, 372 (2005).

[7] S. Catani *et al.*, Phys. Lett. B **269**, 432 (1991), "Durham" jets with the p_T cut-off parameter set at 15 GeV/c.

[8] J. Abdallah *et al.* [DELPHI Collaboration], Eur. Phys. J. C **32**, 185 (2004).

[9] G. Borisov, Nucl. Instrum. Meth. A **417**, 384 (1998).

[10] V. Abazov *et al.* [DØ Collaboration], in preparation for submission to Phys. Rev. D; DØ Note 5029, available from http://www-d0.fnal.gov/Run2Physics/WWW /results/prelim/B/B32/.

[11] T. Sjöstrand *et al.*, Comput. Phys. Commun. **135**, 238 (2001), v6.2.

[12] D.J. Lange, Nucl. Instr. Meth. Phys. Res. A **462**, 152 (2001); for details see http://hep.ucsb.edu/people/lange/EvtGen, v00-07-74.

[13] R. Brun and F. Carminati, CERN Program Library Long Writeup W5013, 1993 (unpublished), v3.15.

[14] H.G. Moser and A. Roussarie, Nucl. Instr. Meth. A **384**, 491 (1997).